MAGNETOHYDRODYNAMICS Vol. 52 (2016), No. 3, pp. 369–377

# EFFECT OF SIZE AND STRETCH OF A MOVING FERROFLUID DROP ON INDUCED ELECTROMOTIVE FORCE

*Ching-Yao Chen*[1,*], *Sheng-Yan Wang*[1],
*Chih-Yung Wen*[2], *Cheng-Shiung Jan*[1]

[1] *Department of Mechanical Engineering, National Chiao Tung University, Hsinchu, Taiwan, Republic of China*
[2] *Department of Mechanical Engineering, Hong Kong Polytechnic University, Hong Kong, China*
[*] *e-Mail: chingyao@mail.nctu.edu.tw*

Application for obtaining useful global features, e.g. the size and stretch of a moving ferrofluid drop by analyzing the characteristics of the induced electromotive force signal is demonstrated. These features are highly relevant to two maximum magnitudes in the electromotive force signal, e.g., the positive ($V_1$) and the negative ($V_2$) peak respectively induced when the drop enters and leaves the region covered by the induction coil. Favorable induction conditions of these two maximum magnitudes are opposite. In general, $V_1$ increases with the size of the ferrofluid drop because of stronger magnetization. On the contrary, $V_2$ is more prominent for a smaller drop, whose stretch is less significant. As a result, the ratio of $|V_1/V_2|$ monotonically increases with the size of the ferrofluid drop. This finding suggests that the induced EMF signal can be used as a useful tool for quantifying the flow conditions, such as the size and stretch of moving ferrofluids.

**Introduction.** Ferrofluid is a remarkable class of smart materials, whose particles are nanometer-sized and coated by surfactants. Conventional applications of ferrofluids in the industry has been well-established, e.g., multistage rotary seals, inertial dampers and loudspeakers [1, 2]. New applications are implemented in micro-technology [3] and materials as well as in biomedicine [4].

On the other hand, it is well known by the Faraday law that the electromotive force (EMF thereafter) is induced in response to unsteady motion of magnetized materials. The induced EMF can be obtained by the Faraday law as

$$\mathrm{EMF} = -N_\mathrm{c}\frac{\mathrm{d}\phi}{\mathrm{d}t}, \tag{1}$$

$$\phi = \int(\mathbf{B}\cdot\mathbf{n})\mathrm{d}A, \tag{2}$$

where $N_\mathrm{c}$, $\phi$, and $t$ stand, respectively, for the number of identical turns of the induction coil, the magnetic flux, and the time. $\mathbf{n}$ and $A$ represent a unit normal vector and the area. The magnetic induction field $\mathbf{B}$ can be further expressed by

$$\mathbf{B} = \mu_0(\mathbf{H}+\mathbf{M}), \tag{3}$$

where $\mu_0$, $\mathbf{H}$ and $\mathbf{M}$ are the permeability of vacuum, the magnetic field strength, and the magnetization of ferrofluids, respectively. It is apparent that both the temporal variations of the magnetic induced field and the effective area, which is perpendicular to the magnetic flux, are able to generate the EMF. Devices for measuring the concentration and dispersion quality of magnetic particles by the induced EMF had been suggested several decades ago [5]. Similar studies but with ferrofluids were conducted both experimentally and theoretically [6].

The reverse situation of liquid motion driven by the interaction of thermoelectric current and magnetic field was also studied [7]. In recent years, new techniques have been proposed to measure the void fractions and velocities of bubbles in the gas–liquid (or gas–ferrofluids) flow system by their electromagnetic induction [8–10]. In addition, understandings of the characteristics of electromagnetic induction are also crucial if an electricity conversion device from the moving magnetic fluids is desired [11, 12]. To gain more fundamental understandings of the electromagnetic induction of moving ferrofluids, experiments for undeformable ferrofluids contained in a small bottle, with a constant velocity were performed [13]. Magnitudes of the induced EMF for various volumes and shapes (i.e. the aspect ratio of containers) of the ferrofluid subjected to different external field strengths are analyzed. The results could be potentially applied to characterize the motion of well-controlled ferrofluids.

In this work, we experiment more practical situations, in which the EMF is induced by a deformable magnetized ferrofluid drop driven by the attraction of permanent magnets. We focus on the influences of relevant physical conditions, such as the external field strength and size of the ferrofluid drop, on the characteristics of the corresponding EMF signal. To elucidate the corresponding behaviors of the ferrofluid drop, parallel experiments with no induction coil are carried out as well, so that the motion of the ferrofluid drop can be clearly observed. The results are expected to provide insight information for flow diagnosis by the EMF signal.

**1. Experimental setup.** The experimental setup consists of a glass tube and an induction coil, as depicted in Fig. 1. The glass tube, whose diameter is 12 mm, is filled with a mixture of glycerol and water to match the density of the experimented ferrofluids. A ferrofluid drop, which is the commercial light mineral oil based ferrofluids (EMG905) produced by the Ferrotec Corp, with volume $\forall_f$, is then placed in the tube above the coil. The ferrofluid drop is pulled downward by the permanent magnets at the bottom of the tube. The number of magnets used in different experiments is denoted by $N$. The tube is placed through the inner

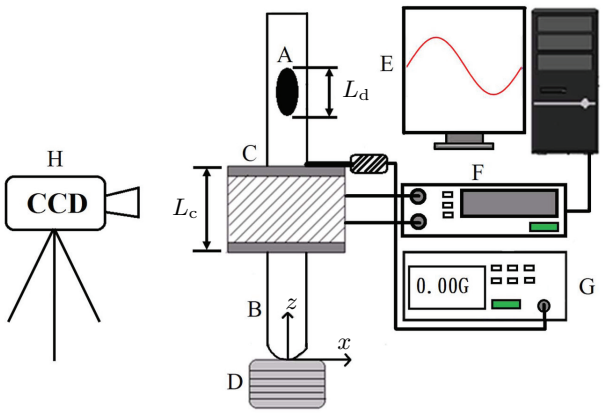


*Fig. 1.* Principle sketch of the experimental setup. A: ferrofluid drop; B: glass tube; C: induction coil; D: magnets; E: personal computer; F: data capturer; G: Gaussmeter; H: CCD camera. $L_d$ and $L_c$ are the longitudinal lengths of the stretched ferrofluid and induction coil, respectively. A ferrofluid drop, initially suspended in a surrounding fluid with identical density, is attracted by magnets to move downward and pass through the induction coil.

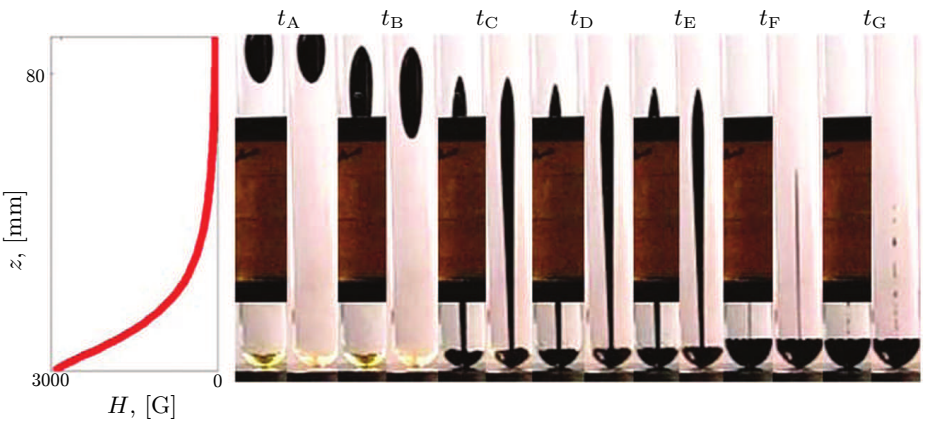


*Fig. 2.* Images of a ferrofluid drop with the volume $\forall_f = 0.40$ ml attracted by six magnets ($N = 6$) at different times $t_A \sim t_G$. Left: the distribution of the external magnetic field strength along the vertical distance, denoted by $z$, away from the magnets. Two experiments with identical conditions with and without the induction coil are respectively demonstrated in the left and right. The case with the induction coil is used to measure the induced EMF, while detailed motion of the ferrofluid drop is observed in the experiment without the induction coil.

hole of the induction coil, whose outer and inner diameters are 78 mm and 15 mm, respectively. The height of the induction coil is $L_c = 51$ mm and has 2160 turns of 0.6 mm-diameter wire. A gaussmeter probe is placed on the top of the coil to record the local magnetic flux density. The measurements of the magnetic flux density and induced EMF are made by a data logger and transmitted directly to a personal computer (PC) for further analysis. With the present experimental setup, images of the moving drop are blocked by the coil so that the parallel experiments without the coil are also conducted to record the images by a CCD camera.

## 2. Results and discussion.

*2.1. Representative cases.* The results of a representative series of various volumes subjected to different magnetic field strengths (or numbers of magnets) are first presented to elucidate the distinct features of the induced EMF signals. Shown in Fig. 2 are the images of a moving ferrofluid drop of $\forall_f = 0.40$ ml attracted by six permanent magnets ($N = 6$) for two experiments with/without the induction coil. Also shown in Fig. 2 is the external magnetic field distribution of the magnets, referred to as the background field hereafter in. The parallel experiment without the induction coil is used for better observations of motion and deformation of the ferrofluid drop. On the other hand, the induced EMF is recorded in the experiment with the coil and shown in Fig. 3. Also Fig. 3 shows the magnetic induction field directly measured by the gaussmeter placed on the top of the induction coil. Subjected to the attraction of the magnets, the initially nearly circular drop is stretched and driven to move downwards. At a reference time $t_A$, when the drop locates sufficiently distant from the top of the coil, the magnetic induction field remains almost the same as the background field. As a result, no significant magnetization and EMF are induced. Because of the greater gradient of the background field as the drop moves further downwards, the stretch of the drop is more prominent when it partially enters the region covered by the coil at $t_B$. In addition, the stronger local field strength enhances the magnetization, so that the measured strength of the magnetic induction field starts to deviate from

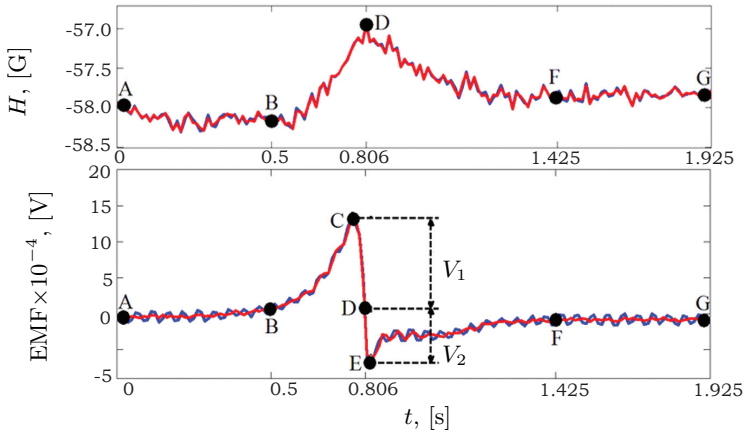


*Fig. 3.* Evolutions of magnetic induction field strength (top) and induced EMF (bottom) for the experiment shown in Fig. 2, i.e. $N = 6$ and $\forall_f = 0.40\,\text{ml}$. Points A $\sim$ G correspond to the times of $t_A \sim t_G$ shown in Fig. 2. The induction field strength is measured on the top of the induction coil as mark G in Fig. 1. The original measured values are plotted by blue curves, and smoothed by FFT filter as shown by the red curves. $V_1$ and $V_2$, which respectively occur at $t_C$ and $t_E$, represent the positive and negative peak EMF magnitudes, respectively.

the background field, and the EMF is induced consequently. The trend keeps evolving, e.g., a more prominent stretch of the drop, a stronger magnetization and induced EMF, until the EMF reaches maximum at $t_C$ denoted as $V_1$. Afterward, the growth rate of the magnetization decreases so that the EMF decays to zero at $t_D$ when the magnetization is in its maximum. The growth rate of magnetization turns negative to induce a negative EMF and reaches its maximum magnitude at $t_E$ denoted as $V_2$. Note that the drop remains highly stretched at $t_D$ and $t_E$. A similar decay of EMF occurs when the negative growth rate of magnetization becomes milder. At $t_F$, almost all the ferrofluids reach the bottom of the tube, and the measured strength of the magnetic induction field returns to nearly background field with no significant induced EMF. We would like to point out that even the general pattern of the EMF signal with maximum positive and negative magnitudes is consistent with the cases discussed in [13], in which the ferrofluids move at a constant velocity without deformation, the present signal does not appear symmetrically, e.g., $|V_1| > |V_2|$. The asymmetry of the EMF signal clearly indicates the strong influences of the unsteady motion and significant stretch of the moving drop to the EMF signal. To further realize the induction signal, a smaller drop subjected to fewer magnets is experimented, e.g., $\forall_f = 0.20\,\text{ml}$ and $N = 3$ shown in Fig. 4, where the total magnetic effects are weaker, e.g., the magnetization strength and the magnetic attraction. It is very interesting to note that a distinct feature of the EMF signal is resulted. Though the asymmetry is still preserved, the maximum magnitude of the EMF appears at the negative peak, i.e. $|V_1| < |V_2|$. To verify the trend, a case with weaker magnetic effects was tested, e.g., $\forall_f = 0.05\,\text{ml}$ and $N = 1$ shown in Fig. 5. A consistent result was obtained allowing to conclude that the ratio between the peak magnitudes of the induced EMF, i.e. $|V_1|/|V_2|$, depends strongly on the magnetic effects. These interesting observations suggest potential applications of the EMF signal to characterize the drop motion.

*2.2. Characterization of the EMF signal.* To better realize the features of the induced EMF signals, the underlined mechanisms for electromagnetic in-

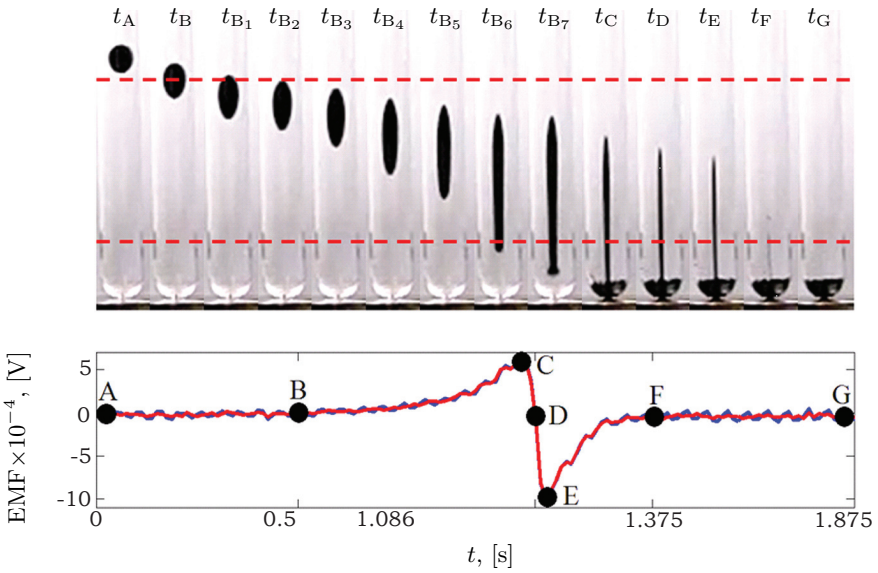


*Fig. 4.* Images of the ferrofluid drop (top) and evolution of the induced EMF (bottom) for $N = 3$ and $\forall_f = 0.20\,\text{ml}$. The induction coil region in the corresponding experiment for obtaining EMF is indicated by red dash lines.

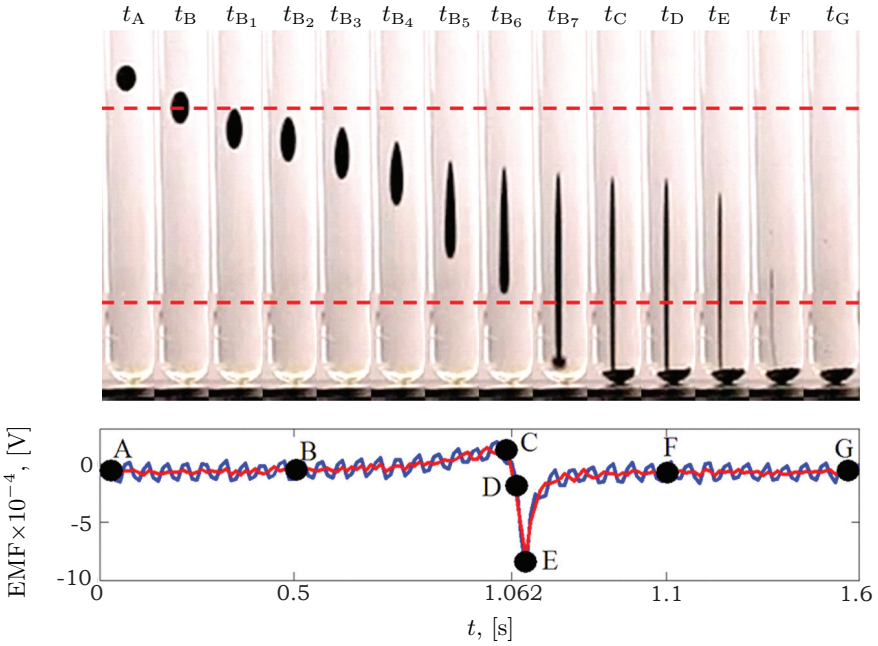


*Fig. 5.* Images of the ferrofluid drop (top) and evolution of the induced EMF (bottom) for $N = 1$ and $\forall_f = 0.05\,\text{ml}$. The induction coil region in the corresponding experiment for obtaining EMF is indicated by red dash lines.

duction are worthy for detailed discussion. According to the Faraday law, the EMF is induced by the unsteady magnetic effects, so that a stronger magnetization is generally favorable. Since the magnetized strength is affected by the local

magnetic field strength and by the volume of magnetized fluids, magnetization is always stronger for a bigger drop approaching closer the magnets. As shown in Figs. 2 and 3, the measured magnetic induction field starts to rise when the drop is about to enter the induction coil at $t_{\mathrm{B}}$ to induce a distinguishable positive EMF. The induced EMF keeps increasing to its maximum $V_1$ at $t_{\mathrm{C}}$ because of more magnetized ferrofluids reaching within and passing through the induction coil. Afterwards, the induced EMF shows a decrease when a major portion of the magnetized fluids leave the region of the coil, so that the EMF opposite sign is induced as the negative peak $V_2$ occurring at $t_{\mathrm{E}}$. The induced EMF eventually vanishes when all the ferrofluids have completely passed through the coil. The overall scenario is generally similar to the cases presented in [13]. Nevertheless, somehow unexpected is a smaller magnitude of the negative peak, i.e. $|V_1| > |V_2|$, since the local background field is stronger at $t_{\mathrm{E}}$ due to the shorter distance away from the magnets. The reason for this unexpected result is attributed to drop deformation, or to the longer stretched length $L_{\mathrm{d}}$ of the drop. As demonstrated in Fig. 2, the magnetic attraction, which is relevant to the field gradient, increases as the drop moves further downward. The drop is highly elongated after $t_{\mathrm{c}}$. This stretched drop results in a milder unsteady effect, or rate, of the local magnetization within the region covered by the coil, so that the magnitude of the induced EMF appears lower though the local magnetization is stronger. This explains the reason of greater magnitudes of the positive induced EMF, i.e. $|V_1| > |V_2|$, for a larger drop with significant stretch. On the other hand, for the smaller drops, e.g., cases shown in Figs. 3 and 4, the positive induced EMFs are lower at the time when the drops enter and pass through the coil because of the weaker effective magnetizations associated with the ferrofluids smaller volumes. Nevertheless, the stretches of these drops are less prominent at the later stage when the drops leave the coil, so that the effective rates of magnetizations for the region covered by the coil are relatively higher. Consequently, the higher induced EMF occurs at the later stage when the ferrofluids leave the coil and the reverse feature of the induced EMF signals is resulted, i.e. $|V_1| < |V_2|$.

The results presented above suggest that the maximum magnitudes of the positive and negative induced EMF are mainly dominated by the volume and by the stretch of the drop, respectively. To further verify the arguments, series of experiments with a fixed background field strength, e.g., $N = 6$, for different drop sizes are presented. Note that multiple experiments were carried out for each conditions, and the results are represented by their means. The corresponding maximum magnitudes of the positive and negative EMF for various values of $\forall_{\mathrm{f}} = 0.05 \sim 0.40\,\mathrm{ml}$ are illustrated in Fig. 6. The maximum positive induced EMFs show the monotonic increase, which is in line with the expectation. As for the negative induced EMFs, the maximum magnitudes increase for cases of relatively small drops, e.g., $\forall_{\mathrm{f}} \leq 0.10\,\mathrm{ml}$, is followed by a decreasing trend for the larger drops, e.g., $\forall_{\mathrm{f}} \geq 0.10\,\mathrm{ml}$. The inconsistency for smaller sizes of the drops ($\forall_{\mathrm{f}} \leq 0.10\,\mathrm{ml}$) can be explained by the domination of magnetization. As mentioned in the previous paragraph, both the positive and the negative inductions, without the influences of the drop stretch, are expected to increase as the volume of the drop becomes larger. For smaller drops, the drop stretch is less prominent, so that the influences on the lower negative induced EMF are less significant. On the other hand, the effects of increasing ferrofluid volume which enhance the induced EMF are relatively more significant. As a result, increasing EMFs are observed associated with larger volumes for the case with relatively smaller sizes of drops, e.g., $\forall_{\mathrm{f}} \leq 0.10\,\mathrm{ml}$. Nevertheless, stretches of the ferrofluids at the later stage which tend to reduce the negative EMFs are more prominent as the drops become bigger,

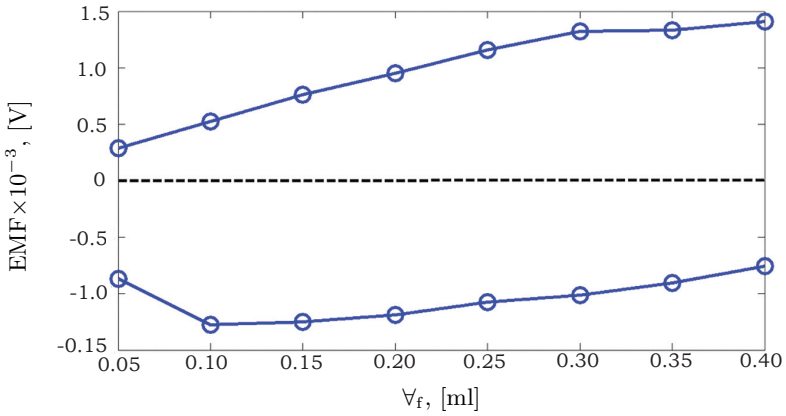


*Fig. 6.* Positive and negative peak EMF values for various volumes of the ferrofluid drop ($\forall_f$) driven by six magnets ($N = 6$).

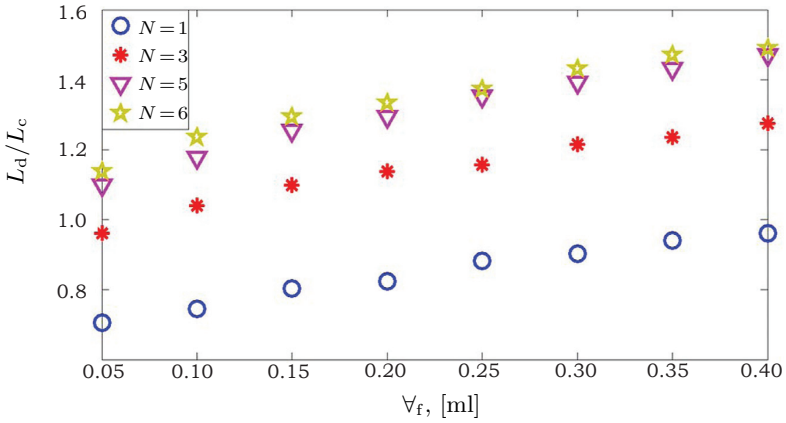


*Fig. 7.* Normalized maximum stretched drop length, denoted as $L_d/L_c$, measured at the time when ferrofluids reach the tube bottom, for different conditions of the drop volumes ($\forall_f$) and number of magnets $N$.

e.g., the stretched length $L_d$ for various drop sizes shown in Fig. 7. When the drop exceeds a certain critical size, the influences of stretches to weaken EMFs would eventually dominate and lead to the decrease of the negative EMFs, as shown for the cases of $\forall_f \geq 0.10\,\text{ml}$. The competition between the stronger magnetization and the prominent stretch of the ferrofluids to the negative EMFs explains the non-monotonic behavior illustrated in Fig. 6.

For the cases reported above, we conclude that the features of the EMF signals, e.g., the maximum magnitudes of the positive and negative EMFs, are highly relevant to the drop conditions, such as the original sizes and the stretched behaviors during the motion. For many practical conditions when observations of flow fields are difficult, it would be beneficial if the forth mentioned global flow conditions, e.g., the sizes of moving ferrofluids, can be obtained by analyzing the easy-accessed EMF signals. Shown in Fig. 8 are the ratios of the peak magnitudes of EMF signals ($|V_1/V_2|$) for different sizes of ferrofluid drops. An interesting monotonic increase of the ratio is obtained. This monotonic trend is the aftermath of the arguments discussed above. On the one hand, a larger drop is always associated with a stronger magnetization to result in a higher $|V_1|$ at early stage

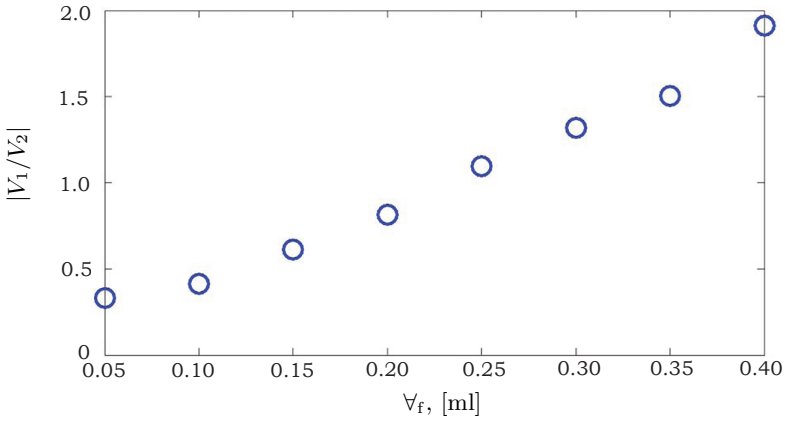


*Fig. 8.* The ratio of positive and negative peak EMF values ($|V_1/V_2|$) for different volumes of the ferrofluid drop ($\forall_f$) driven by six magnets ($N = 6$).

in which the stretch is not prominent. On the other hand, the larger drop tends to result in a prominent stretch at later stage to reduce $|V_2|$. Consequently, the value of $|V_1/V_2|$ would monotonically increase with the volume of the ferrofluid drop.

**3. Concluding remarks.** In this work, we experimentally study the characteristics of the electromagnetic induction of a magnetized ferrofluid drop attracted by magnets to pass through an induction coil. To better observe the motion of the drop, parallel experiments under identical conditions without the induction coil are also carried out. Because of acceleration and deformation when the drop approaches the magnets, the signal of the induced electromotive force appears to be asymmetric. This asymmetry of the EMF signal provides useful information for potential flow diagnosis. We focus on the maximum magnitudes of EMF signals, e.g., the positive ($V_1$) and the negative ($V_2$) peak value, respectively induced at the early and late stages. The magnitude of ($V_1$) is predominated by the magnetization strength which increases with the size of the ferrofluid drop. On the contrary, the magnitude of ($V_2$) is weakened if the stretch is prominent, which is favorable for a larger drop. As a result, the ratio of $|V_1/V_2|$ increases monotonically with the size of the ferrofluid drop. This fact provides very useful information for quantifying the global flow conditions by analyzing the EMF signal, such as the size and the stretch of the moving ferrofluid drop.

**Acknowledgments.** Support by the Ministry of Science and Technology of the Republic of China (Taiwan) under grant MOST No. 104-2221-E-009-142-MY3 is acknowledged. C.-Y. Wen is supported by the Research Grants Council, Hong Kong under Contract No. GRF PolyU 152168/14E.

## References

[1] R.E. Rosensweig. *Ferrohydrodynamics* (Cambridge University Press, Cambridge, England, 1985).

[2] E.Y. Blums, A.O. Cebers, M.M. Maiorov. *Magnetic Fluids* (Walter de Gruxter, New York, 1997.)

[3] N.T. Nguyen. Micro-magnetofluidics: interactions between magnetism and fluid flow on the microscale. *Microfluid Nanofluid*, vol. 12 (2012), pp. 1–16.

[4] C. Scherer and A.M. Figueiredo Neto. Ferrofluids: properties and applications. *Brazilian Journal of Physics*, vol. 35 (2005), pp. 718–727.

[5] T.M. Kwon, M.S. Jhon, and T.E. Karis. A device for measuring the concentration and dispersion quality of magnetic particle suspensions. *IEEE Transactions on Instrumentation and Measurement,*, vol. 41 (1992), , no. 1, pp. 10–16.

[6] A.A. Kubasov. Electrmotive force generation due to ferrofluid motion. *Journal of Magnetism and Magnetic Materials,*, vol. 193 (1997), pp. 15–19.

[7] I. Kaldre, Y. Fautrelle, J. Etay, A. Bojarevics and L. Buligins. Investigation of liquid phase motion generated by the thermoelectric current and magnetic field interaction. *Magnetohydrodynamics*, vol. 46 (2010), no. 4, pp. 371–380.

[8] S. Shuchi, H. Yamaguchi and M. Takemura. Measurement of void fraction in magnetic fluid using electromagnetic induction. *J. Fluids Eng.*, vol. 125 (2003), p. 479.

[9] T. Kuwahara, and H. Yamaguchi. Void fraction measurement of gas-liquid two-phase flow using magnetic fluid. *J. Thermophys. Heat Transf.*, vol. 21 (2007), p. 173.

[10] T. Kuwahara, F. De Vuyst, and H. Yamaguchi. Bubble velocity measurement using magnetic fluid and electromagnetic induction. *Phys. Fluids*, vol. 21 (2009), pp. 097101.

[11] F. Gazeau, C. Baravian, J.-C. Bacri, R. Perzynski, and M.I. Shliomis. Energy conversion in ferrofluids: magnetic nanoparticles as motors or generators. *Phys. Rev. E*, vol. 56 (1997), pp. 614–18.

[12] S. Carcangiu, A. Montisci and R. Pintus. Performance analysis of an inductive MHD generator. *Magnetohydrodynamics,* vol. 48 (2012), no. 1, pp. 115–124.

[13] C.-Y. Chen, S.-Y. Wang, C.-M. Wu, C.-H. Lin, and K.-A. Huang. Characteristics of electromagnetic induction by moving ferrofluids. *Magnetohydrodynamics,* vol. 48 (2012), no. 3, pp. 567–580.

Received 07.01.2016